REPORT

Changes in groundwater storage represent a significant source of atmospheric CO_2 in China

Quanzhou Li,[1,2] Yun Pan,[1,2,*] Chong Zhang,[1,2] Qingquan Zhang,[1,2] Changqing Li,[3] Huan Huang,[3] and Huili Gong[1,2]

*Correspondence: pan@cnu.edu.cn

Received: March 23, 2024; Accepted: September 4, 2024; Published Online: September 26, 2024; https://doi.org/10.59717/j.xinn-geo.2024.100094

GRAPHICAL ABSTRACT

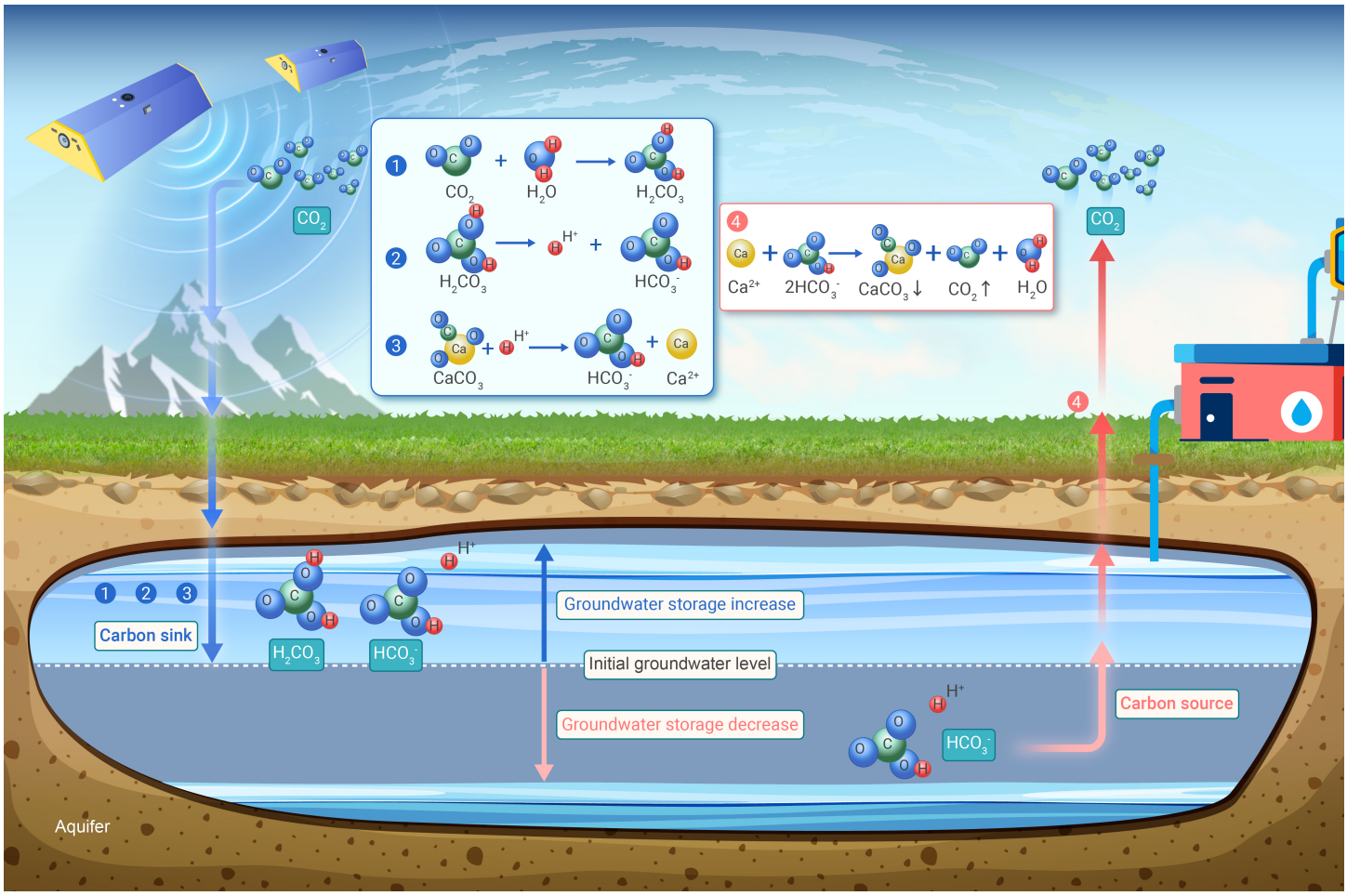

PUBLIC SUMMARY

- The CO_2 emission due to groundwater storage change in China is estimated to be 2.1±2.3 Mt/yr in 2003–2015.
- Groundwater storage change exceeds 15% emission sources listed in China Carbon Emission Accounts and Datasets.
- China's groundwater overdraft control will lead to a total reduction of 5.3 Mt CO_2 by 2025.

REPORT

Changes in groundwater storage represent a significant source of atmospheric CO_2 in China

Quanzhou Li,[1,2] Yun Pan,[1,2,*] Chong Zhang,[1,2] Qingquan Zhang,[1,2] Changqing Li,[3] Huan Huang,[3] and Huili Gong[1,2]

[1]Beijing Laboratory of Water Resources Security, Capital Normal University, Beijing 100048, China
[2]College of Resources Environment and Tourism, Capital Normal University, Beijing 100048, China
[3]China Institute for Geo–Environmental Monitoring, Beijing 100081, China
*Correspondence: pan@cnu.edu.cn

Received: March 23, 2024; Accepted: September 4, 2024; Published Online: September 26, 2024; https://doi.org/10.59717/j.xinn-geo.2024.100094

Citation: Li Q., Pan Y., Zhang C., et al., (2024). Changes in groundwater storage represent a significant source of atmospheric CO_2 in China. The Innovation Geoscience **2(4)**: 100094.

Recent studies show that groundwater depletion is an unreported source of atmospheric CO_2 through bicarbonate reactions in the groundwater released from aquifer. However, the depletion can be mitigated or offset by recharge, and thus the contrasting roles of depletion and recharge on carbon cycle remain unclear at a national scale. Here, we extend previous studies to use the satellite–derived groundwater storage change (GWSC) and substantial in situ measurements of the bicarbonate ion concentration (BIC), for the first time evaluation of GWSC–induced CO_2 emission/sequestration in China. Results show that the GWSC represents as a significant source of atmospheric CO_2 in China, with a net CO_2 emission rate of 2.1±2.3 Mt/yr, which is larger than 15% of the emission sources listed in China Carbon Emission Accounts and Datasets. Besides, emission and sequestration induced by groundwater storage (GWS) decrease and increase is also significant, with a rate of 3.9±1.1 Mt/yr and 1.8±1.2 Mt/yr, respectively. Notably, we also find that China's stricter groundwater measures can contribute a total reduction of 5.3 Mt CO_2 emission in the major overdraft areas by 2025. Despite of notable uncertainties, this study highlights the unneglectable contributions of GWSC to atmospheric CO_2 emission and sequestration at a national to global scale.

INTRODUCTION

Groundwater is a crucial component of terrestrial water cycle[1] and is closely related to the physical exchange and chemical transformation of carbon between rivers and the atmosphere, exhibiting significant spatial and temporal dynamics.[2,3] The complex interactions between different earth spheres and the relationships between carbon cycling and biogeochemical processes highlights the need of an improved understanding of groundwater contributions to the carbon cycling.[4–6] Current carbon cycling studies related to hydrology primarily focus on surface water bodies such as oceans, rivers, wetlands, and reservoirs, while less investigations are made for groundwater.[7–11] Previous studies mainly focus on three kinds of processes related to groundwater carbon cycling: dissolved CO_2 degassing and sequestration,[12,13] rock–water reactions absorbing atmospheric CO_2,[14,15] and CO_2 emissions from energy consumption for agriculture irrigation.[16–18]

Besides, groundwater–related carbon cycle is also associated with the bicarbonate reactions.[19] This reactions can be forward or back. Forward reactions involve atmospheric CO_2 deposition and rock weathering, where CO_2 is absorbed through groundwater recharge. In contrast, when groundwater is released to the atmosphere, the exposed groundwater will reequilibrate in a back reaction and the CO_2 will be released to atmosphere with other minerals to form carbonate and silicate rocks. In the North China Plain (NCP), excessive groundwater overdraft has led to drastic GWS decrease since the 1990s.[20] Estimates suggest that the total CO_2 emissions induced by groundwater depletion in the NCP may is about 0.5 Mt/yr.[21,22] In the United States, Wood and Hyndman et al. (2017) estimated atmospheric CO_2 emissions from GWS depletion of the US to be 1.7 Mt/yr.[23] A following study by Mishra et al. (2018) demonstrated a total CO_2 emission of 0.72 Mt/yr from the areas with long–term GWS depletion.[24] Although the estimates are much smaller in comparison to some major sources, they remain noticeable, e.g., it is equal to or greater than approximately one third of the 23 major sources in the US.

However, in the studies by Wood & Hyndman (2017) and Mishra et al. (2018),[23,24] only groundwater depletion is considered for the emission. Since CO_2 sequestration happens when dissolved inorganic carbon (DIC) downwards into groundwater through recharge,[25] the exclusive use of groundwater depletion in above studies fail to revealing contrasting roles of groundwater storage change (GWSC) in carbon cycle, and thus limits the understanding of groundwater's contribution to carbon neutrality.[26] A recent study shows that groundwater depletion is widespread but not universal. According to their statistics, there are nearly 30% of the selected global aquifers were experiencing reversed declining or continuous rising in groundwater levels.[27] In China, although the NCP has been identified as one of the area with severe groundwater depletion,[20,28,29] a recent study shows that increasing GWS are observed in 7 of the 18 major aquifers in China.[30] The contrasting trends of GWSC highlights the potential conflicts of GWSC in carbon source and sink over a larger region.

Whether the GWSC can be regarded as a carbon source or sink at a regional scale, depends on the combined effects of GWSC and concentration of bicarbonate ions (BIC). Due to limited data on spatially distributed GWSC and BIC, the GWSC at a national scale has been little investigated to demonstrate whether it is a carbon source or sink. Although the Gravity Recovery and Climate Experiment (GRACE) satellites have been increasingly used to quantify regional GWSC,[31,32] the uncertainties remain noticeable.[30,33] Besides, adequate in situ measurements of BIC are also helpful for reliable BIC, which may lead to significant impact on estimated CO_2 emission.[24]

This study, for the first time, extends previous studies to evaluate GWSC–induced CO_2 emission and sequestration in China, by using GWSC derived from ensemble GRACE estimates from 3,456 combinations and the BIC measured at 10,163 in situ monitoring wells. The major motivation of this study is to explore the contributions of GWSC to atmospheric CO_2 emission and sequestration in China, especially focusing on whether it is a carbon source or sink considering both GWS increase and decrease. We will first introduce the principles of GWSC–induced atmospheric CO_2 emission and sequestration, and the methods for estimation. Then, we will discuss the results related to GWSC–induced CO_2 emission and sequestration, as well as its implications for national and global carbon neutrality.

MATERIALS AND METHODS

Principles of GWSC–induced atmospheric CO_2 emission and sequestration

Figure 1 illustrates the reactions of the inorganic carbon cycle in groundwater. Groundwater recharge from precipitation is in equilibrium with atmospheric CO_2. The recharging groundwater increases GWS and rapidly equilibrates to the higher concentration forming hydrogen and bicarbonate ions.[23,34] Thus, the forward reactions associated with GWS increase results in the removal of atmospheric CO_2, as represented by Equations (1), (2), and (3). In contrast, when groundwater is released to the atmosphere due to natural or anthropogenic discharge, the exposed groundwater will reequilibrate with the atmospheric pressure and the CO_2 will be released to atmosphere with other minerals to form carbonate and silicate rocks.[23,35] The back reactions are represented with Equation (4). The detailed reactions are described as following.

The atmospheric CO_2 enters the subsurface through groundwater recharge, and the dissolved CO_2 in groundwater forms carbonic acid (Equation (1)):

$$CO_2+H_2O \rightarrow H_2CO_3. \quad (1)$$

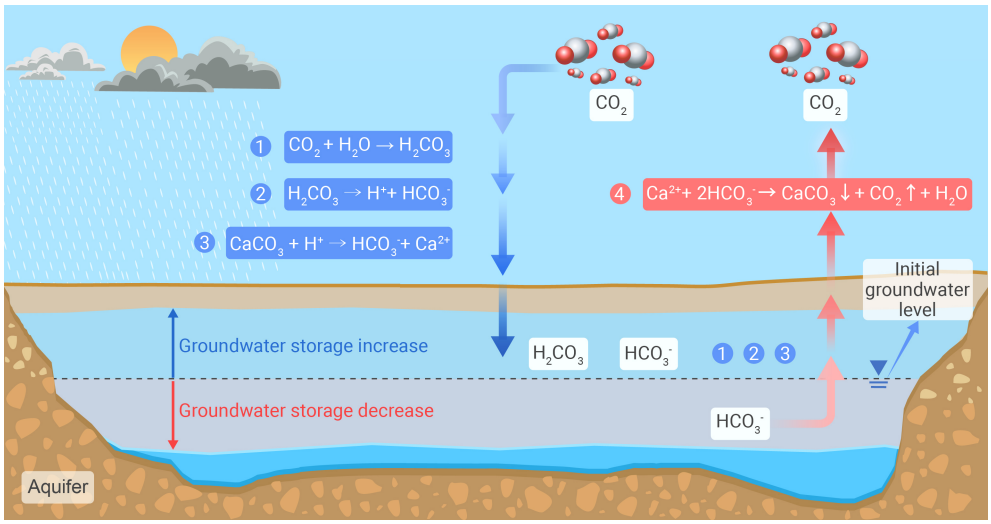

Figure 1. Schematic diagram illustrating the reaction mechanisms between GWSC and inorganic carbon cycling in groundwater.

However, the carbonic acid is unstable and decomposes into hydrogen ions and bicarbonate (Equation (2)):

$$H_2CO_3 \rightarrow H^+ + HCO_3^-. \quad (2)$$

In the aquifer, the abundant presence of calcite reacts with hydrogen ions to generate bicarbonate (Equation (3)):

$$CaCO_3 + H^+ \rightarrow HCO_3^- + Ca^{2+} \quad (3)$$

Due to natural discharge or anthropogenic pumping of groundwater, the pressure of the exposed groundwater decreases and the reaction reverses to balance the atmospheric pressure (Equation (4)):

$$Ca^{2+} + 2HCO_3^- \rightarrow CaCO_3\downarrow + CO_2\uparrow + H_2O \quad (4)$$

Therefore, the GWSC–induced atmospheric CO_2 emission (sequestration) can be expressed with Equation (5):

$$m(CO_2) = 1/2 \times GWSC \times S \times c(CO_2) \quad (5)$$

Where, $m(CO_2)$ represents the amount of CO_2 emission (sequestration); S represents the area corresponding to GWSC; $c(CO_2)$ represents the equivalent concentration of CO_2 in groundwater. Referring to previous studies by Wood and Hyndman et al. (2017) and Mishra et al. (2018),[23,24] we conservatively estimate that half of the bicarbonate entering the atmosphere is converted into CO_2. The emission and sequestration refers to negative and positive GWSC, respectively.

Ensemble estimation of GWSC using GRACE data

To solve GWSC, we used three GRACE Tellus Level–3 products and three Mascon solutions provided by the Center for Space Research (CSR), German Research Centre for Geosciences (GFZ), and Jet Propulsion Laboratory (JPL) to derive monthly terrestrial water storage change data. Non–GWSC components of water storage (including surface water storage, soil moisture storage, snow water equivalent, and canopy water storage) were obtained using two global hydrological models (PCR–GLOBWB 2 and WGHM), three land surface models (CLSM–F2.5, NOAH–3.6, and VIC 4.1.2 from GLDAS–2.1), and the ERA5–land reanalysis product. The data were collected monthly from January 2003 to 2015 and resampled to a uniform spatial resolution of 1° × 1° to match GRACE data. Additionally, we used the degree–day model glacier dataset[36] and the global glacier mass loss dataset from the early 21st century[37] to estimate monthly–scale glacier water equivalent change in China from 2003 to 2015, with the spatial resolution resampled to 1°×1°. The GWSC is calculated with Equation (6):

$$GWSC = TWSC - SWSC - SMSC - SWEC - CWSC - GWEC \quad (6)$$

where, TWSC represents terrestrial water storage change; SWSC represents surface water storage change; SMSC represents soil moisture storage change; SWEC represents snow water equivalent change; CWSC represents canopy water storage change; and GWEC represents glacier water equivalent change.

All the non–GWSC compartments in Equation (6) were converted to monthly anomalies by subtracting the 2003–2015 mean from the original time series, to be consistent with GRACE GWSC. The GWSC in this study is same as the widely used groundwater storage anomaly (GWSA). We prefer to use GWSC instead of GWSA as it is the change of GWS contributes to CO_2 emission and sequestration. Thus, the positive value of GWSC means that it is larger than the 2003–2015 mean. That is to say, the positive GWSC does not definitely mean an increasing trend of GWS, it can also be decreasing if the deceasing rate is smaller than the 2003–2015 mean. It should be noted that Hainan and Taiwan were excluded from the analysis to avoid notable leakage errors from the ocean in GRACE data.

There will be a total of 3,456 GWSC solutions considering the different sources of the GRACE and non–GWSC datasets. The use of different datasets in estimating GWSC can better reflect its uncertainties. The Bayesian Model Average (BMA) method is then used to integrate different solutions for a robust GWSC estimation.[38] The BMA has been widely used in GRACE–era.[39,40] It uses the prior knowledge to integrate multiple different models by assigning weights, and then merge them to get a new GWSC, which not only reflects the common characteristics of the solutions, but also synthesizes the advantages of different solutions. It thus provides relative reliable probability distribution of all the results.

The GWSC estimated by using CSR mascon, WGHM, and the average of two glacier dataset is selected as the reference model in BMA. The CSR mascon and WGHM are selected as they have been widely used and well demonstrated in previous studies, while the two glacier dataset is averaged to account for their different ways in estimating glacier mass change (i.e., modeling and remote sensing). The periods of 2003–2011 and 2012–2015 is used for BMA calibration and merging, respectively. The weight ratios of GWSC ensembles are adjusted at each grid cell in the study area. The optimal GWSC solution is obtained by multi–source merging of all GWSC solutions from 2003 to 2015 based on the weight ratios. For more details, please refer to Li et al. (2023).[33]

Estimation of carbon storage changes due to groundwater storage change

The hydrochemical characteristics of groundwater in China mainly comprise heavy bicarbonate water and a mixture of heavy bicarbonate sulfate chloride water, accounting for 87% of the total area. Bicarbonate ion water constitutes approximately half of the national area. Detailed information on the hydrochemical types of groundwater in China can be found on the official website of the Geological Cloud (https://geocloud.cgs.gov.cn/). In this study, we used BIC data from 10,163 wells monitored throughout the year in 2019 as part of the National Groundwater Monitoring Project, where various groundwater quality indicators were measured once a year. Using the Inverse Distance Weighting (IDW) interpolation method, we interpolated all data points to a spatial resolution of 1° × 1° to match the spatial resolution of annual GWSC trend. Subsequently, we obtained the 1° gridded CO_2 emission (sequestration) induced by GWSC in China from 2003 to 2015 according to Equation (5).

Uncertainty analysis

We considered the uncertainties introduced by different models and conducted an uncertainty analysis of the GWSC and CO_2 emission (sequestration) induced by GWSC using the standard deviation (STD) based on BMA merging. That is to say, we calculated the standard deviation of GWSC and

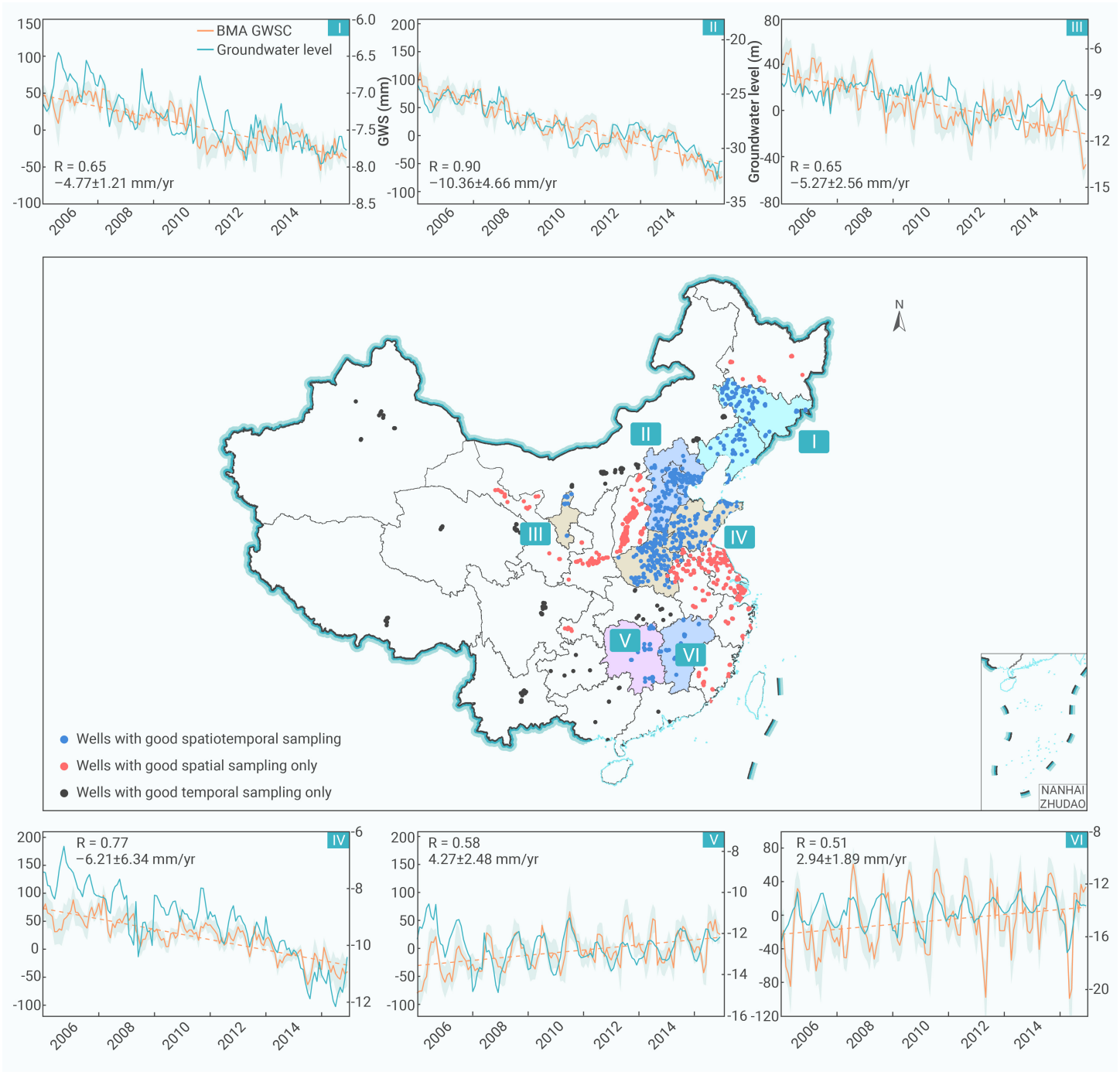

Figure 2. Comparison of GRACE–derived GWSC and well–observed groundwater level data in six typical regions of China Six regions are numbered as I–VI, which correspond to Jilin and Liaoning, Beijing, Tianjin and Hebei, Ningxia, Shandong and Henan, Hunan, Jiangxi respectively.

CO_2 emission (sequestration) induced by GWSC at the grid scale and aggregated it to province scale. The standard deviation was used to represent the uncertainty. Additionally, during the comparison with the measured water level in wells, we first obtained the monthly time series of BMA–merged GWSC and then calculated the standard deviation month by month to represent the uncertainty of its monthly time series.

RESULTS AND DISCUSSIONS

Validation of GRACE GWSC using well observations

Since reliable aquifer storage coefficients are generally not available, we compare the GRACE–derived GWSC with in situ groundwater level changes for validation purpose (Figure 2). Considering the data quality of in situ measurements, we only select the wells that evenly distributed within a region and have little missing records (Type I), while the other wells that have notable missing records (Type II) and poorly distributions (Type III) are not used for validation. Thus, we only compare them in the six selected sub–regions, i.e., I–Jilin and Liaoning, II–Beijing, Tianjin, and Hebei, III–Ningxia, IV–Shandong and Henan, V–Hunan, and VI–Jiangxi. To address the impact of spatial coverage limitations on the GWSC validation, we constructed Thiessen Polygons (Figure S1) based on the distribution of the wells and used the area–weighted results to be compared with the long–term GWSC time series.

The results show good correlations between the GRACE–GWSC and the measured groundwater level data in the six regions (I–VI). The highest correlation coefficient is 0.9 in region II, while the correlation coefficients for the remaining regions range from 0.51 to 0.77. The better performance in region II ascribes to the sufficient wells and good temporal coverage of the data. Despite that the data limitations of in situ measurements may degrade the

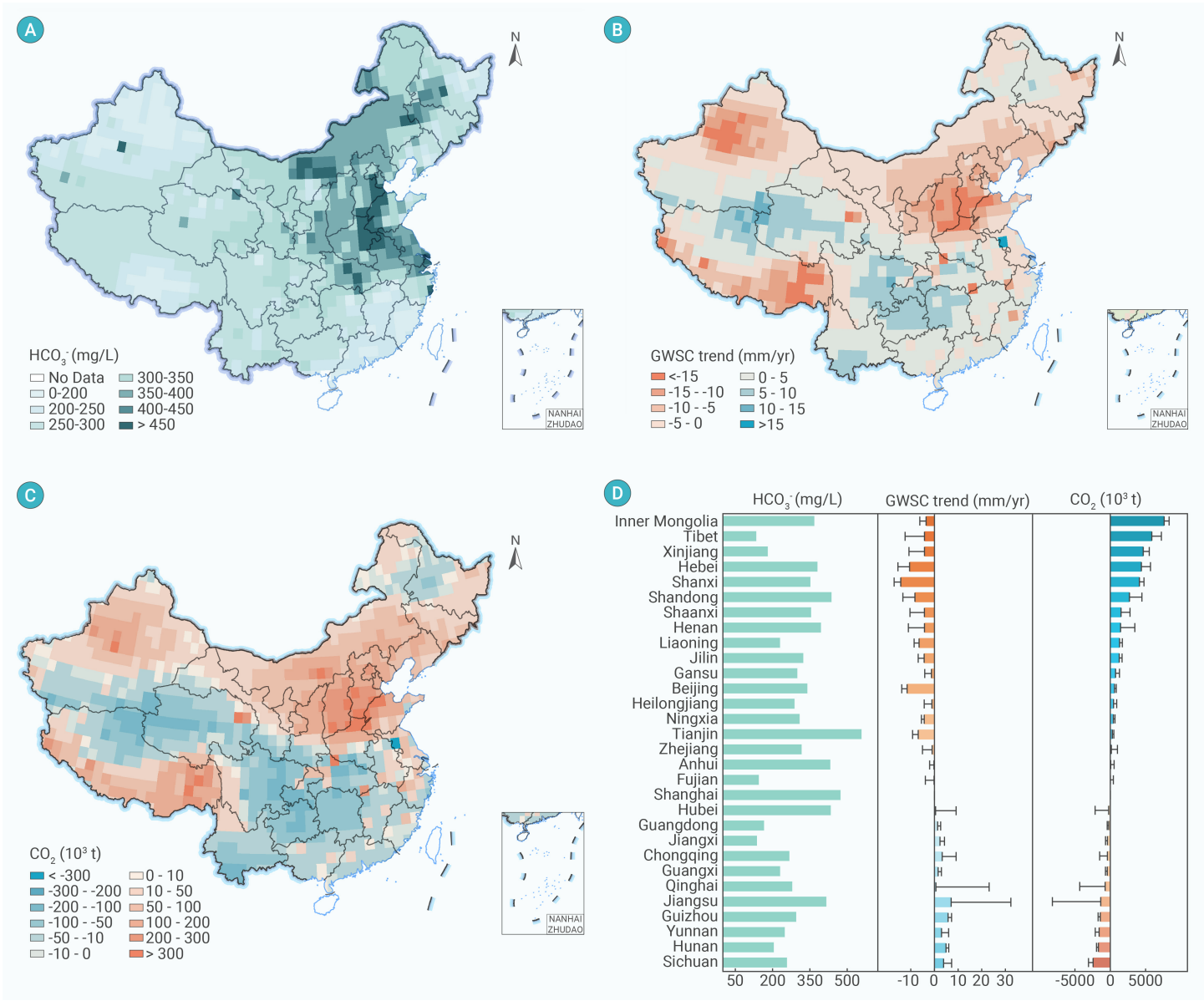

Figure 3. Distribution of groundwater BIC, annual GWSC trend, and the total CO_2 emission (A) Spatial distribution of groundwater BIC in China collected by the National Groundwater Monitoring Project. The gridded BIC data are derived from 10,163 in situ observations after IDW interpolation. (B) Spatial distribution of 2003–2015 annual GWSC trend estimated GRACE–based BMA merging. (C) Spatial distribution of total CO_2 emission (or sequestration) calculated by the combination of BIC and annual GWSC trend data in China. (D) Three bar charts (from left to right) show the BIC, annual GWSC trend, and the total CO_2 emission (sequestration), respectively, in 30 major provinces of China.

comparison performance, our estimates are in consistent with previous studies in other regions. For example, the decreasing trend in region I (−5.27 ± 2.56 mm/yr) is similar to the findings of Zhong et al. (2018) (−6.76 ± 3.2 mm/yr),[41] the decreasing trend in region IV (−6.21 ± 6.34 mm/yr) is comparable to that of Su et al., (2020) (−11.4 ± 8.9 mm/yr),[42] and the increasing trends in regions V and VI are consistent with that by Yin et al. (2021) (1.55 mm/yr).[43] The other regions with little or without in situ monitoring data also show comparable estimates with previous studies (e.g., Yin et al., 2021; Yi et al., 2016; Zhao et al., 2023).[43–45]

The hotspots of severe GWS decrease in the northwest, southwest, and North China account for half of the total GWS decrease in China (Figure 3B). The GWS decrease in the northwest and North China is mainly driven by human activities.[45] The GWS decrease in the southeastern Qinghai–Tibet Plateau probably ascribes to decreased precipitation, but further investigations are still need.[46–48] Additionally, the GWS increase in central China is attributed to climate change with increasing precipitation[49] and human–induced alterations in the hydrological cycle, where intensive surface water irrigation has contributed to increased land water storage, subsequently replenishing groundwater levels in the central and southeastern parts of the Yangtze River basin.[50]

CO_2 emission and sequestration induced by GWSC in China

Figure 3A shows that the BIC in groundwater is higher in North and East China in comparison to the western and southern regions. This variation is attributed to the geological conditions of the aquifers and the degree of dissolution and reaction of atmospheric CO_2 after entering groundwater.[51] The average groundwater BIC in China is 320 mg/L. Tianjin has the highest BIC (557.5 mg/L) among the focused provinces, while Tibet is the lowest (134.2 mg/L). The BIC in other provinces ranges between 136.8 and 473.1 mg/L. Northern China is predominantly composed of sandy soil, providing better conditions for ion exchange in groundwater, whereas southern regions are dominated by clay soil, resulting in weaker ion exchange capacity.[52] The western regions, influenced by complex groundwater chemical types and low precipitation,[53,54] have relative lower BIC in groundwater with an average of 157 mg/L.

Figure 3B shows the overall GWSC trend of China is −1.93 ± 4.5 mm/yr during 2003–2015, while the GWS decrease and increase is −3.55 ± 1.98 mm/yr and 1.62 ± 2.16 mm/yr, averaged over the areas with increasing and decreasing GWSC trend, respectively. The net CO_2 emission associated with the overall depletion trend is 2.1 ± 2.3 Mt/yr (Figure 3C). While the CO_2 emission and sequestration associated with the decreasing and increasing GWSC

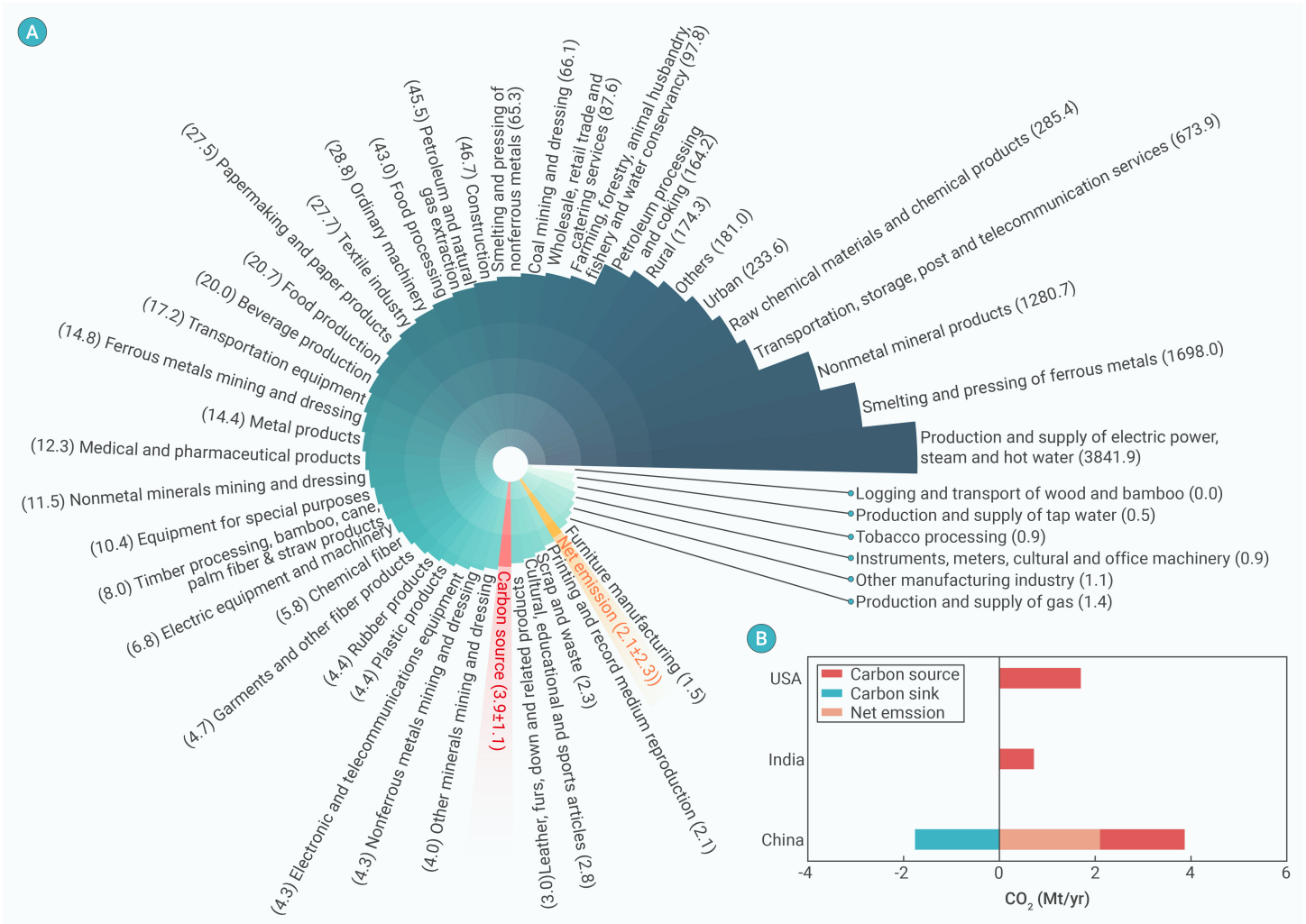

Figure 4. China's GWSC–induced CO_2 emission (A) Schematic diagram showing the ranking of China's GWSC–induced CO_2 emission (unit: Mt) among 47 CO_2 emission sectors in 2015. The numbers in parentheses represent the CO_2 emission from relevant sectors. (B) Comparison of the GWSC–induced CO_2 emission (sequestration) in China with that in United States and India. Note that in China the carbon source represents the annual CO_2 emission induced by the decrease of GWS, while the carbon sink represents the annual CO_2 sequestration induced by the increase of GWS. The net emission represents the annual net CO_2 emission induced by overall GWSC considering both increase and decrease.

trend is 3.9 ± 1.1 Mt/yr and −1.8 ± 1.2 Mt/yr, respectively. The GWSC–induced carbon source areas are mainly found in the northern, northwestern, and southeastern Qinghai–Tibet Plateau of China. While the GWSC–induced carbon sink areas are mainly found in the central–western and southern regions.

Province scale statistics show that there are 18(12) provinces represent carbon source (sink) area regarding the negative (positive) GWSC trend (Figure 3D). Inner Mongolia has the largest total CO_2 emission from 2003 to 2015 (7634.2 ± 694.2 × 10^3 t), while the emissions in other carbon source provinces range from 10.7 ± 426 × 10^3 t in Fujian to 5883.0 ± 1352.7 × 10^3 t in Tibet. However, it should be noted that the larger emissions in Inner Mongolia, Xinjiang, and Tibet mainly ascribes to its larger size in area, rather than the larger GWSC trend. In contrast, despite of smaller size in area, provinces in North China (including Shanxi, Beijing, Tianjin, Hebei, Henan, and Shandong) exhibit more significant GWS depletion and thus also result in notable CO_2 emissions. Similarly, the total CO_2 sequestration during 2003–2015 varies among provinces in response to the area and GWSC trend, with the maximum sequestration (−2426.0 ± 650.3 × 10^3 t) in Sichuan and minimum sequestration in Hubei (−231.2 ± 1914.6 × 10^3 t). The higher uncertainty in Jiangsu, Qinghai, and Hubei ascribes to larger deviations in GWSC estimates due to surface water storage change.

Since the GWSC represents a seasonal cycle, we further estimated the associated CO_2 emission and sequestration in seasonal variations (Figure S2). It shows that summer season represents carbon sink due to GWS increase, leading to a sequestration of 10.2 Mt CO_2 from May to August. In contrast, other months represent carbon source due to GWS decrease, leading to an emission of 11.7 Mt CO_2. The more notable emission and sequestration due to GWSC at seasonal scale highlights the significant contributions of GWSC to carbon storage changes within the year.

The implications for carbon neutrality

We compared the CO_2 emissions induced by GWSC with other major emission sources in China listed in the Carbon Emissions Accounts and Dataset (CEADs) in 2015.[55] Based on the emission inventory of 47 sectors (Figure 4A), there are significant differences in annual CO_2 emissions across various sectors in China, ranging from nearly 0 Mt of Logging and Transport of Wood and Bamboo to 3842 Mt of the Production and Supply of Electric Power, Steam, and Hot Water. It shows that the annual CO_2 emissions (3.9 ± 1.1 Mt/yr) due to GWS decrease is larger than 25% of the emissions from all 47 sectors in China. The net GWSC (i.e., considering both GWS decrease and increase) remains a notable source of emissions (2.1±2.3 Mt/yr) that is larger than 15% of the all 47 sectors. These comparisons highlight the significance of atmospheric CO_2 emissions resulting from GWSC.

Since emission is largely regulated by the GWSC, we investigated how stricter groundwater measures can affect the GWSC–induced CO_2 emission. According to the '14th Five–Year Plan' for Groundwater Overexploitation in Key Areas (http://www.mwr.gov.cn/), there will be a total reduction of 4.6 billion m^3 in groundwater abstraction in the 10 key overdraft regions (161,000 km^2) by 2025. These areas account for 56% of the national overdraft area and nearly 70% of China's total groundwater overdraft. Given an average BIC of 320 mg/L, this reduction in groundwater abstraction can lead to a decrease of 5.3 Mt of CO_2 emission. This amount is comparable to the

planned emission reductions of other sectors as reported by CEADs[56] from 2005–2019, which includes reductions of 5.2 Mt, 5.2 Mt, 5.5 Mt, and 5.3 Mt in the Chemical Fiber, Smelting and Pressing of Ferrous Metals, Smelting and Pressing of Nonferrous Metals, and Metal Products sectors, respectively. The notable reduction of CO_2 emission induced by groundwater overdraft control in comparison with other solutions, highlights the significance of stricter groundwater measures in carbon neutrality in China.

In comparison with previous studies (Figure 4B), the GWSC–induced net CO_2 emission in China (2.1 ± 2.3 Mt/yr) is larger than that in US (1.7 Mt/yr) and India (0.72 Mt/yr). A major reason for the difference ascribes to the larger BIC (320 mg/L) derived from 10,163 in situ monitoring wells collected in our study, which is much larger than the national averaged one (190 mg/L) in US. However, it should be noted that the CO_2 emission (3.9 ± 1.1 Mt/yr) due to GWS decrease will be much larger than that reported in the US and India. This probably ascribes to the different data source of GWSC used in our study (i.e., GRACE–based) in comparison with that in the US (model–based) and India (in situ–based).

We further made a global investigation regarding the GWSC contributions to carbon neutrality. According to the global groundwater depletion rate of 100–200 Gt/yr,[57–59] an emission of GWSC–induced CO_2 at global scale can be estimated to be 11.5–23 Mt/yr given an average BIC of 320 mg/L based on our data. This estimates is larger than previously reported one (8–17 Mt/yr), which was calculated based on an average BIC (190 mg/L) of the US. Critically, previous study generally focused on the degassing in groundwater, and found that global groundwater abstraction can lead to an emission of 0.01–0.03 Pg C/yr (or 37–110 Mt CO_2/yr).[13] Our estimates indicate that the total (i.e., degassing pluses reaction) global CO2 emissions from groundwater can be one quarter larger than previously reported one that only focuses on degassing.

Additionally, it is noteworthy that this study reveals the contrasting roles of GWSC in carbon emission and sequestration. Given a global groundwater recharge rate (12,000–17,000 km^3/yr),[60] we estimated that the CO_2 sequestration due to GWSC–induced reactions is 1.4–2.0 Gt/yr, which is comparable to but slightly larger than previous estimates (0.73 Gt/yr) considering the global flux of DIC downward into groundwater. The difference mainly ascribes to that the in situ measured BIC is used in our study while the estimated DIC is used in previous study. Despite of large uncertainties in global estimates, this study highlights that groundwater represents a significant contribution to global CO_2 emission and sequestration.

Limitations of this study

In this study, we estimated the CO_2 emission and sequestration due to the reactions associated with GWSC in China. However, the carbon cycle related to groundwater is much more complicated than we discussed above. For example, we did not consider about the degassing in groundwater,[61] as well as the energy consumption related with groundwater pumping.[62] Besides, dissolved organic carbon also plays an important role in the carbon cycle.[63] The exclusive considering of these processes may greatly limit our estimates to be much insignificant while referring to emissions caused by GWSC. Thus, it should be noted that this study is not to provide an estimates of total CO_2 emissions due to degassing, reaction, energy consumption, organic materials, and other processes related to groundwater.

Besides, notable uncertainties may exist in our estimates due to the bias in GWSC and BIC data. The GRACE–estimated GWSC can be greatly impacted by the errors in satellite measurements and non–GWS data.[30,33] The in situ measured BIC from 10,163 monitoring wells also remains uncertain due to its limited sampling in space and time. The relative short study period (2003–2015) also limits our understanding for a longer time span. Notably, the assumption of half of bicarbonate in groundwater all participate in the reaction may overestimate the emissions as parts of irrigated groundwater can reenter into aquifers through infiltration.

CONCLUSIONS

This study estimated the CO_2 emission and sequestration due to reactions related with GWSC in China by using the GWSC derived from GRACE and BIC from 10,163 monitoring wells. In contrast to previous studies, it quantifies both the CO_2 emission and sequestration induced by GWSC and thus reveals the contrasting roles of GWSC in affecting atmospheric CO_2 dynamics. The major findings result from this study include:

(1) GWSC in China represents a source of atmospheric CO_2 with an emission rate of 2.1 ± 2.3 Mt/yr during 2003–2015, which is larger than 15% of the emission types listed in the CEADs.

(2) The net emission consists of a source of 3.9 ± 1.1 Mt/yr and a sink of 1.8 ± 1.2 Mt/yr CO_2 due to GWS decrease and increase, respectively.

(3) A preliminary estimation based on literature and data collected from this study shows that the CO_2 emission from global groundwater depletion is 11.5–23 Mt/yr, while China's groundwater overdraft control will lead to a total reduction of 5.3 Mt CO_2 by 2025.

REFERENCES

1. Famiglietti, J.S. (2014). The global groundwater crisis. Nat. Clim. Change **4**: 945–948. DOI: 10.1038/nclimate2425.
2. Battin, T.J., Lauerwald, R., Bernhardt, E.S., et al. (2023). River ecosystem metabolism and carbon biogeochemistry in a changing world. Nature **613**: 449–459. DOI: 10.1038/s41586-022-05500-8.
3. Wang, C., Brennwald, M.S., Xie, Y., et al. (2023). Quantifying carbon cycling across the Groundwater-Stream-Atmosphere Continuum using High-Resolution time series of multiple dissolved gases. Environ. Sci. Technol. **57**: 13487–13495. DOI: 10.1021/acs.est.3c03378.
4. Falkowski, P., Scholes, R.J., Boyle, E., et al. (2000). The global carbon cycle: A test of our knowledge of Earth as a system. Science **290**: 291–296. DOI: 10.1126/science.290.5490.291.
5. Monger, H.C., Kraimer, R.A., Khresat, S.e., et al. (2015). Sequestration of inorganic carbon in soil and groundwater. Geology **43**: 375–378. DOI: 10.1130/g36449.1.
6. Wallmann, K. and Aloisi, G. (2012). The Global Carbon Cycle: Geological Processes. In Fundamentals of Geobiology, A. H. Knoll, D. E. Canfield, and K. O. Konhauser, eds. (Wiley), In pp. 20-35. DOI: 10.1002/9781118280874.ch3.
7. de Klein, J.J.M. and van der Werf, A.K. (2014). Balancing carbon sequestration and GHG emissions in a constructed wetland. Ecol. Eng. **66**: 36–42. DOI: 10.1016/j.ecoleng.2013.04.060.
8. Keller, P.S., Marcé, R., Obrador, B., et al. (2021). Global carbon budget of reservoirs is overturned by the quantification of drawdown areas. Nat. Geosci. **14**: 402–408. DOI: 10.1038/s41561-021-00734-z.
9. Gruber, N., Bakker, D.C.E., DeVries, T., et al. (2023). Trends and variability in the ocean carbon sink. Nat. Rev. Earth Environ. **4**: 119–134. DOI: 10.1038/s43017-022-00381-x.
10. Le, T.P.Q., Marchand, C., Ho, C., et al. (2018). CO_2 partial pressure and CO_2 emission along the lower Red River (Vietnam). Biogeosciences **15**: 4799–4814. DOI: 10.5194/bg-15-4799-2018.
11. Duan, H., Xiao, Q., and Qi, T. (2023). Measuring lake carbon dioxide from space: Opportunities and challenges. The Innovation Geoscience **1**: 100025. DOI: 10.59717/j.xinn-geo.2023.100025.
12. Lawter, A.R., Qafoku, N.P., Asmussen, R.M., et al. (2017). Risk of geologic sequestration of CO_2 to groundwater aquifers: Current knowledge and remaining questions. Energy Procedia **114**: 3052–3059. DOI: 10.1016/j.egypro.2017.03.1433.
13. Macpherson, G.L. (2009). CO_2 distribution in groundwater and the impact of groundwater extraction on the global C cycle. Chem. Geol. **264**: 328–336. DOI: 10.1016/j.chemgeo.2009.03.018.
14. Liu, Z., Dreybrodt, W., and Wang, H. (2008). A possible important CO_2 sink by the global water cycle. Chinese Science Bulletin **53**(3): 402–407. DOI: 10.1007/s11434-008-0096-9.
15. Hartmann, J., Jansen, N., Dürr, H.H., et al. (2009). Global CO_2-consumption by chemical weathering: What is the contribution of highly active weathering regions. Glob. Planet. Change **69**: 185–194. DOI: 10.1016/j.gloplacha.2009.07.007.
16. Rothausen, S.G.S.A. and Conway, D. (2011). Greenhouse-gas emissions from energy use in the water sector. Nat. Clim. Change **1**: 210–219. DOI: 10.1038/nclimate1147.
17. Wang, J., Rothausen, S.G.S.A., Conway, D., et al. (2012). China's water–energy nexus: Greenhouse-gas emissions from groundwater use for agriculture. Environ. Res. Lett. **7**: 014035. DOI: 10.1088/1748-9326/7/1/014035.
18. Qin, J., Duan, W., Zou, S., et al. (2024). Global energy use and carbon emissions from irrigated agriculture. Nat. Commun. **15**: 3084. DOI: 10.1038/s41467-024-47383-5.
19. Liu, Z. and Dreybrodt, W. (2015). Significance of the carbon sink produced by H_2O–carbonate–CO_2–aquatic phototroph interaction on land. Sci. Bull. **60**: 182–191. DOI: 10.1007/s11434-014-0682-y.
20. Gong, H., Pan, Y., Zheng, L., et al. (2018). Long-term groundwater storage changes and land subsidence development in the North China Plain (1971–2015). Hydrogeol. J. **26**: 1417–1427. DOI: 10.1007/s10040-018-1768-4.
21. Leng, P., Li, F., Du, K., et al. (2020). Flow velocity and nutrients affect CO_2 emissions from agricultural drainage channels in the North China Plain. Environ. Sci. Eur. **32**: 146. DOI: 10.1186/s12302-020-00426-2.
22. Zhang, Z., Shi, D., Ren, F., et al. (1997). Evolution of Quaternary groundwater system in North China Plain. Sci. China Earth Sci. **40**: 276–283. DOI: 10.1007/BF02877536.
23. Wood, W.W. and Hyndman, D.W. (2017). Groundwater depletion: A significant unreported source of atmospheric carbon dioxide. Earth's Future **5**: 1133–1135. DOI: 10.1002/2017EF000586.

24. Mishra, V., Asoka, A., Vatta, K., et al. (2018). Groundwater depletion and associated CO_2 emissions in India. Earth's Future **6**: 1672–1681. DOI: 10.1029/2018EF000939.
25. Kessler, T.J. and Harvey, C.F. (2001). The global flux of carbon dioxide into groundwater. Geophys. Res. Lett. **28**: 279–282. DOI: 10.1029/2000GL011505.
26. Dong, S., Liu, B., Lei, J., et al. (2022). Carbon balance model of groundwater system –A field application. J. Hydrol. **610**: 127845. DOI: 10.1016/j.jhydrol.2022.127845.
27. Jasechko, S., Seybold, H., Perrone, D., et al. (2024). Rapid groundwater decline and some cases of recovery in aquifers globally. Nature **625**: 715–721. DOI: 10.1038/s41586-023-06879-8.
28. Zhang, C., Duan, Q., J.-F. Yeh, P., et al. (2021). Sub-regional groundwater storage recovery in North China Plain after the South-to-North water diversion project. J. Hydrol. **597**: 126156. DOI: 10.1016/j.jhydrol.2021.126156.
29. Pan, Y., Zhang, C., Gong, H., et al. (2017). Detection of human-induced evapotranspiration using GRACE satellite observations in the Haihe River basin of China. Geophys. Res. Lett. **44**: 190–199. DOI: 10.1002/2016GL071287.
30. Yang, J., Pan, Y., Zhang, C., et al. (2024). Comparison of groundwater storage changes over losing and gaining aquifers of China using GRACE satellites, modeling and in-situ observations. Sci. Total Environ. **938**: 173514. DOI: 10.1016/j.scitotenv.2024.173514.
31. Rodell, M., Famiglietti, J.S., Wiese, D.N., et al. (2018). Emerging trends in global freshwater availability. Nature **557**: 651–659. DOI: 10.1038/s41586-018-0123-1.
32. Rodell, M. and Reager, J.T. (2023). Water cycle science enabled by the GRACE and GRACE-FO satellite missions. Nature Water **1**: 47–59. DOI: 10.1038/s44221-022-00005-0.
33. Li, Q., Pan, Y., Zhang, C., et al. (2023). Quantifying multi-Source uncertainties in GRACE-Based estimates of groundwater storage changes in mainland China. Remote Sens. **15**: 2744. DOI: 10.3390/rs15112744.
34. Wan Isahak, W.N.R., Che Ramli, Z.A., Mohamed Hisham, M.W., et al. (2015). The formation of a series of carbonates from carbon dioxide: Capturing and utilisation. Renew. Sustain. Energy Rev. **47**: 93–106. DOI: 10.1016/j.rser.2015.03.020.
35. Dreybrodt, W., Eisenlohr, L., Madry, B., et al. (1997). Precipitation kinetics of calcite in the system $CaCO_3$ H_2O CO_2: The conversion to CO_2 by the slow process $H^+ + HCO_3^- \rightarrow$ CO2+H2O as a rate limiting step. Geoch. Cosm. Act. **61**: 3897–3904. DOI: 10.1016/S0016-7037(97)00201-9.
36. Wu, Yanan and Pan, Yun (2021). Estimating glacial material balance in the Asian high sierra 1999–2019 using Degree-Day models and gravity satellites. Master's thesis, Capital Normal University.
37. Hugonnet, R., McNabb, R., Berthier, E., et al. (2021). Accelerated global glacier mass loss in the early twenty-first century. Nature **592**: 726–731. DOI: 10.1038/s41586-021-03436-z.
38. Duan, Q., Ajami, N.K., Gao, X., et al. (2007). Multi-model ensemble hydrologic prediction using Bayesian model averaging. Adv. Water Resour. **30**: 1371–1386. DOI: 10.1016/j.advwatres.2006.11.014.
39. Long, D., Pan, Y., Zhou, J., et al. (2017). Global analysis of spatiotemporal variability in merged total water storage changes using multiple GRACE products and global hydrological models. Remote Sens. Environ. **192**: 198–216. DOI: 10.1016/j.rse.2017.02.011.
40. Jia, B., Cai, X., Zhao, F., et al. (2020). Potential future changes of terrestrial water storage based on climate projections by ensemble model simulations. Adv. Water Resour. **142**: 103635. DOI: 10.1016/j.advwatres.2020.103635.
41. Zhong, Y., Zhong, M., Feng, W., et al. (2018). Groundwater depletion in the west Liaohe river basin, China and its implications revealed by GRACE and in situ measurements. Remote Sens. **10**: 493. DOI: 10.3390/rs10040493.
42. Su, Y., Guo, B., Zhou, Z., et al. (2020). Spatio-Temporal variations in groundwater revealed by GRACE and its driving factors in the Huang-Huai-Hai Plain, China. Sensors **20**: 922. DOI: 10.3390/s20030922.
43. Yin, Z., Xu, Y., Zhu, X., et al. (2021). Variations of groundwater storage in different basins of China over recent decades. J. Hydrol. **598**: 126282. DOI: 10.1016/j.jhydrol.2021.126282.
44. Yi, S., Wang, Q., and Sun, W. (2016). Basin mass dynamic changes in China from GRACE based on a multibasin inversion method. J. Geophys. Res. Solid Earth **121**: 3782–3803. DOI: 10.1002/2015JB012608.
45. Zhao, K., Fang, Z., Li, J., et al. (2023). Spatial-temporal variations of groundwater storage in China: A multiscale analysis based on GRACE data. Resour. Conserv. Recycl. **197**: 107088. DOI: 10.1016/j.resconrec.2023.107088.
46. Zhang, G., Yao, T., Shum, C.K., et al. (2017). Lake volume and groundwater storage variations in Tibetan Plateau's endorheic basin. Geophys. Res. Lett. **44**: 5550–5560. DOI: 10.1002/2017GL073773.
47. Zou, Y., Kuang, X., Feng, Y., et al. (2022). Solid water melt dominates the increase of total groundwater storage in the Tibetan Plateau. Geophys. Res. Lett. **49**: e2022GL100092. DOI: 10.1029/2022GL100092.
48. Feng, W., Shum, C.K., Zhong, M., et al. (2018). Groundwater storage changes in China from satellite gravity: An overview. Remote Sens. **10**: 674. DOI: 10.3390/rs10050674.
49. Long, D., Yang, Y., Wada, Y., et al. (2015). Deriving scaling factors using a global hydrological model to restore GRACE total water storage changes for China's Yangtze River Basin. Remote Sens. Environ. **168**: 177–193. DOI: 10.1016/j.rse.2015.07.003.
50. Huang, Y., Salama, M.S., Krol, M.S., et al. (2015). Estimation of human-induced changes in terrestrial water storage through integration of GRACE satellite detection and hydrological modeling: A case study of the Yangtze River basin. Water Resour. Res. **51**: 8494–8516. DOI: 10.1002/2015WR016923.
51. Zhu, Q., Li, X., Jiang, Z., et al. (2015). Impacts of CO_2 leakage into shallow formations on groundwater chemistry. Fuel Process. Technol. **135**: 162–167. DOI: 10.1016/j.fuproc.2014.11.042.
52. Liu, F., Zhang, G.-L., Song, X., et al. (2020). High-resolution and three-dimensional mapping of soil texture of China. Geoderma **361**: 114061. DOI: 10.1016/j.geoderma.2019.114061.
53. Jianhua, S., Qi, F., Xiaohu, W., et al. (2009). Major ion chemistry of groundwater in the extreme arid region northwest China. Environ. Geol. **57**: 1079–1087. DOI: 10.1007/s00254-008-1394-x.
54. Piao, S., Ciais, P., Huang, Y., et al. (2010). The impacts of climate change on water resources and agriculture in China. Nature **467**: 43–51. DOI: 10.1038/nature09364.
55. Shan, Y., Guan, D., Zheng, H., et al. (2018). China CO_2 emission accounts 1997–2015. Sci. Data **5**: 170201. DOI: 10.1038/sdata.2017.201.
56. Shan, Y., Huang, Q., Guan, D., and Hubacek, K. (2020). China CO_2 emission accounts 2016–2017. Sci. Data **7**: 54. DOI: 10.1038/s41597-020-0393-y.
57. Konikow, L.F. (2011). Contribution of global groundwater depletion since 1900 to sea-level rise. Geophys. Res. Lett. **38**: L17401. DOI: 10.1029/2011GL048604.
58. Wada, Y., van Beek, L.P.H., Sperna Weiland, F.C., et al. (2012). Past and future contribution of global groundwater depletion to sea-level rise. Geophys. Res. Lett. **39**: L09402. DOI: 10.1029/2012GL051230.
59. Hasan, M.F., Smith, R., Vajedian, S., et al. (2023). Global land subsidence mapping reveals widespread loss of aquifer storage capacity. Nat. Commun. **14**: 6180. DOI: 10.1038/s41467-023-41933-z.
60. Kuang, X., Liu, J., Scanlon, B.R., et al. (2024). The changing nature of groundwater in the global water cycle. Science **383**: eadf0630. DOI: 10.1126/science.adf0630.
61. Huo, P. and Gao, P. (2024). Degassing of greenhouse gases from groundwater under different irrigation methods: A neglected carbon source in agriculture. Agric. Water Manag. **301**: 108941. DOI: 10.1016/j.agwat.2024.108941.
62. Lal, R. (2004). Carbon emission from farm operations. Environ. Int. **30**: 981–990. DOI: 10.1016/j.envint.2004.03.005.
63. McDonough, L.K., Andersen, M.S., Behnke, M.I., et al. (2022). A new conceptual framework for the transformation of groundwater dissolved organic matter. Nat. Commun. **13**: 2153. DOI: 10.1038/s41467-022-29711-9.

FUNDING AND ACKNOWLEDGMENTS

This research was funded by National Natural Science Foundation of China (No. 42071397, 41771456, 42201345), the Second Tibetan Plateau Scientific Expedition and Research Program (STEP, No. 2019QZKK0207), the Strategic Priority Research Program of the Chinese Academy of Sciences (No. XDA19090120), and the Natural Science Foundation of Beijing Municipality (No. 8232021). The funders had no role in study design, data collection and analysis, decision to publish or preparation of the manuscript.

AUTHOR CONTRIBUTIONS

Y. P. designed the research plan. Q. L. and C. Z. performed the analysis and plotted figures. Y. P., Q. L. and Q. Z. drafted and revised the manuscript. H. H., C. L. and H. G. provided the comments and revised the manuscript. All authors read and approved the final manuscript.

DECLARATION OF INTERESTS

The authors declare no competing interests.

DATA AND CODE AVAILABILITY

The groundwater BIC data reported in this study were provided by the China Institute for Geo-Environmental Monitoring. For information on GEACE and its derived data, please refer to the study of Li et al. (2023).[33]

SUPPLEMENTAL INFORMATION

It can be found online at https://doi.org/10.59717/j.xinn-geo.2024.100094

LEAD CONTACT WEBSITE

Yun Pan: https://cret.cnu.edu.cn/szdw/js/103421.htm